Electrochimica Acta 178 (2015) 494–503

Contents lists available at ScienceDirect

Electrochimica Acta

journal homepage: www.elsevier.com/locate/electacta

Hydrogen diffusivity measurement and microstructural characterization of Custom 465 stainless steel

S. Ifergane[a,b], E. Sabatani[b], B. Carmeli[b], Z. Barkay[c], V. Ezersky[d], O. Beeri[b], N. Eliaz[a,*]

[a] Department of Materials Science and Engineering, Tel-Aviv University, Ramat Aviv, Tel Aviv 6997801, Israel
[b] Nuclear Research Center Negev, Beer Sheva, Israel
[c] The Wolfson Applied Materials Research Centre, Tel-Aviv University, Ramat Aviv, Tel Aviv 6997801, Israel
[d] Ilse Katz Institute for Nanoscale Science and Technology, Ben-Gurion University, Beer-Sheva, Israel

ARTICLE INFO

Article history:
Received 10 March 2015
Received in revised form 4 August 2015
Accepted 4 August 2015
Available online 7 August 2015

Keywords:
Hydrogen diffusion
Hydrogen permeation
Effects of strain
Precipitation hardening stainless steel
Custom 465

ABSTRACT

Hydrogen diffusivity in Custom 465® martensitic precipitation hardened stainless steel is determined using electrochemical permeation tests. Hydrogen diffusivity in the solution annealed (SA) condition is approximately 10 times higher than in the aged H900 (480 °C, 4 h) condition because of hydrogen traps such as Ni_3Ti nano-precipitates and reverted austenite. The microstructure of the alloy is characterized by TEM, XRD and ESEM/EBSD, both in the aged H900 and in the SA conditions. In the aged condition, η-Ni_3Ti nano-precipitates with hexagonal structure and a rod-like shape are observed. In addition, reverted austenite is found at grain boundaries and inter-lath interfaces. In the SA condition, these microstructural features are not evident, which may explain the higher diffusivity measured. The diffusivity is almost unaffected by prior microplastic deformation of H900.

1. Introduction

Carpenter Technology's Custom 465® stainless steel (UNS S46500) [1–3] is a martensitic, age-hardenable alloy that offers a unique combination of high strength, toughness, and corrosion resistance. An ultimate tensile strength higher than 250 ksi (1722 MPa) can be obtained following aging at 482 °C (the H900 condition). However, the H900 condition is characterized by higher susceptibility to corrosion and stress corrosion cracking (SCC) compared to other conditions associated with aging at higher temperatures [4,5].

The microstructure of Custom 465® stainless steel in the solution annealed (SA) condition consists of Fe-Ni lath martensite (BCC phase) [6–7]. As reported for other precipitation hardened stainless steels [8–11], large prior austenite grains are divided into "packets" that are subdivided into "blocks" of martensite laths. When an austenite grain shears under martensitic transformation, there are altogether 24 potential orientations of martensite (variants) that are formed from a single austenite grain. Each packet of lamellae is actually a single martensite variant.

For Custom 465® stainless steel it was reported [6–7] that during the aging treatments, η-Ni_3Ti coherent nano-precipitates are formed inside the martensite lamellae. Reverted austenite is formed between lamella, although its amount was not quantified. The precipitation behavior and the strengthening mechanism in other corrosion-resistant maraging steels have been investigated [12–13]. η-Ni_3Ti precipitates have hexagonal crystallographic structure and a rod-like shape. The size of the precipitates is governed by the time and temperature of the aging treatment. Strengthening by η-Ni_3Ti in the early stage of precipitation is due to coherency stresses and internal ordering.

Not much is known about the sensitivity of Custom 465® to hydrogen embrittlement (HE). Lee and Gangloff [14] compared this sensitivity to HE of AerMet™ 100. It was reported that, in the H900 condition, the fracture mode changes from ductile trans-granular to intergranular, due to hydrogen charging. Based on trends in other precipitation hardened (PH) stainless steels [15–23], it is speculated that the sensitivity to hydrogen is severe in the H900 condition.

In the current work, we used the electrochemical hydrogen permeation technique [24] in order to: (1) Characterize hydrogen diffusivity in Custom 465® stainless steel. (2) Compare between specimens in the SA condition and in the aged H900 condition, in order to determine the effect of aging on hydrogen diffusivity. (c) Study the effect of prior deformation, which is common in high-stress engineering applications, on hydrogen permeation.

* Corresponding author.
E-mail address: neliaz@tau.ac.il (N. Eliaz).

http://dx.doi.org/10.1016/j.electacta.2015.08.016
0013-4686/

2. Experimental procedure

2.1. Thermomechanical treatments and microstructure characterization of Custom 465®

Custom 465® stainless steel in the form of a 2-inch diameter rod was purchased from Carpenter Technology (Wyomissing, PA, USA). The composition of this steel (wt.%) was determined by Inductively Coupled Plasma Atomic Emission Spectroscopy (ICP-AES) analysis as: Fe–10.7Cr–10.9Ni–0.86Mo–1.4Ti–0.04Al–0.04Zn–0.0046C. The rod was received in the SA and cold-treated condition. The SA treatment was done at 982°C for 1 h, followed by rapid cooling to room temperature in either air or a liquid coolant. A subzero cooling at −73°C for 8 h within 8 h from the SA treatment is essential for optimal aging response [3]. Specimens were cut in the transverse direction. Three specimen types were tested: (1) ***SA***: Solution annealed condition, (2) ***H900***: Aged at 482°C for 4 h in argon shielding atmosphere, followed by cooling in argon, and (3) ***deformed H900***: simulating prior deformation effects of already aged components in service. These specimens were aged to H900 and afterwards were subjected to 0.18-0.23% uniaxial deformation, which is close to the yield point in the microplastic deformation region. The degree of deformation was evaluated by a finite element analysis model, in which the plastic strain field generated in uniaxial tension of thin sheet specimen was computed using ABAQUS/explicit 6.1 software.

The microstructure was characterized by scanning electron microscope (SEM), electron backscattered diffraction (EBSD), and X-ray diffraction (XRD). Specimens were ground on SiC papers down to 600 grit, followed by polishing down to 1 μm using diamond polish paste. For metallographic characterization, chemical etching was done by immersion in Villela's reagent, which consists of 5 mL HCl + 2 g picric acid + 100 mL methyl alcohol. For EBSD examinations, specimens were prepared by polishing with colloidal silica to remove the stressed surface layer, followed by electrochemical etching in 64% phosphoric acid + 15% sulfuric acid + 21% water (volume percentages) solution at 3 V for 2 s.

SEM examination was done by Quanta 200 FEG ESEM from FEI. For EBSD analyses, a HKL-Oxford Channel 5 system with Nordlys II detector was used. The following operation conditions were maintained: working distance 15 mm, inclination relative to the main beam 70°.

Three specimens from each type were characterized by XRD, each specimen was tested three times: before hydrogen charging, immediately after charging, and one day later. XRD patterns were acquired 1 h after the end of the electrochemical permeation test, thus ensuring that the specimens were still charged with hydrogen. Data were collected on Panalytical Empyrean Powder Diffractometer equipped with a position sensitive (PSD) PIXCEL detector and a graphite monochromator on the diffracted beam providing Cu-Kα radiation. The operation conditions were: 40 kV and 30 mA. The Bragg-Brentano diffractometer was employed. θ/2θ scans were run for 30 min in a 2θ range of 40-95 deg with steps equal to ~0.033 deg. The relative quantities of reverted austenite were analyzed by Rietveld analysis using FullProof software.

Samples for transmission electron microscopy (TEM) study were mechanically polished to a 100-μm thickness on a 1000 grit SiC grinding paper and polished with 6 μm and 1 μm diamond pastes. The central area of the disk sample was dimple grinded to 20 μm thickness and then ion-milled to electron transparency using Gatan precision ion polishing system (PIPS). TEM and selected area electron diffraction (SAED) experiments were carried out in a JEOL JEM-2100F TEM equipped with an energy-dispersive X-ray spectrometer (EDS) system model JED 2300T. The acquisition parameters were: probe size of 1 nm, acquisition time 20 s, 138 eV resolution.

2.2. Electrochemical hydrogen permeation tests

Electrochemical hydrogen permeation tests were performed in order to determine the diffusion coefficient, permeability and hydrogen subsurface concentration for a given charging condition. The technique was developed by Devanathan and Stachurski [24], and later described in detail elsewhere [25–28]. The experimental setup is described in Fig. 1a. It is comprised of a two-compartment cell, with the specimen being a membrane separating the two compartments. System validation was done with Pd–0.1 wt.%Pt specimens, comparing the results to reported values [29].

For the permeation tests, specimens were ground to a thickness of 0.125–0.2 mm in the same manner described above. The proper specimen thickness range was determined empirically. For too high specimen thicknesses, the experiment durations are too long. On the other hand, an insufficient thickness does not comply with the required thickness of at least 5 grains or packets of banded martensite [24]. In a case where this requirement is not complied with, hydrogen may diffuse through grain boundaries, bypassing transport through the grains. In order to avoid edge effects that cause significant hydrogen leakage laterally, the L/r ratio (where L is the membrane thickness and r is the radius of the surface area exposed to the catholyte) was kept below 0.03. For a reliable measurement, with minimal leakage, this ratio should be less than 0.05 [24,25]. For each sample type, three specimens were tested in various thicknesses, in order to avoid surface and undesired size effects [24].

In the final preparation step prior to the onset of the permeation test, the surface oxide film was removed by polishing with a 1-μm diamond paste. Afterwards, specimens were rinsed in detergent, washed in water, ultrasonically cleaned in acetone, dried quickly in high-pressure air stream, washed in ethanol, and dried in high-

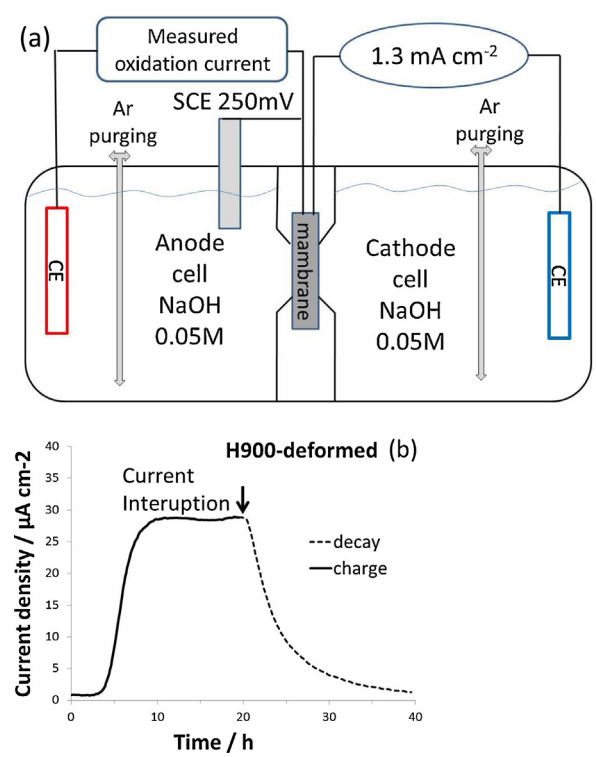

Fig. 1. (a) Schematic illustration of the electrochemical permeation cell assembly. (b) Electrochemical hydrogen permeation charging and decay transients.